

## Theoretical study of lowlying electronic states of $\text{CoH}^+$

J. Anglada, P. J. Bruna, and F. Grein

Citation: *The Journal of Chemical Physics* **92**, 6732 (1990); doi: 10.1063/1.458258

View online: <http://dx.doi.org/10.1063/1.458258>

View Table of Contents: <http://scitation.aip.org/content/aip/journal/jcp/92/11?ver=pdfcov>

Published by the AIP Publishing

---

### Articles you may be interested in

[A theoretical study of the electronic structure and spectroscopic properties of the low-lying electronic states of the molecule SiB](#)

*J. Chem. Phys.* **107**, 6782 (1997); 10.1063/1.474920

[Theoretical study of the electronic spectrum of the CoH molecule](#)

*J. Chem. Phys.* **99**, 1215 (1993); 10.1063/1.465365

[A theoretical study of lowlying electronic states of aminonitrene, phosphinonitrene, and phosphinocarbene](#)

*J. Chem. Phys.* **94**, 8029 (1991); 10.1063/1.460137

[A theoretical investigation of the lowlying electronic states of the molecule  \$\text{BeH}^+\$](#)

*J. Chem. Phys.* **94**, 7237 (1991); 10.1063/1.460207

[Theoretical study of lowlying states of  \$\text{H}\_3\text{O}\$](#)

*J. Chem. Phys.* **91**, 2376 (1989); 10.1063/1.456995

---



# Theoretical study of low-lying electronic states of $\text{CoH}^+$

J. Anglada,<sup>a)</sup> P. J. Bruna,<sup>b)</sup> and F. Grein<sup>c)</sup>

Department of Chemistry, University of New Brunswick, Bag Service No. 45222, Fredericton, New Brunswick E3B 6E2, Canada

(Received 8 September 1989; accepted 13 February 1990)

Potential energy curves and spectroscopic parameters of several electronic states of  $\text{CoH}^+$  have been calculated using multireference configuration interaction methods. The four lowest-lying states  $X^4\Phi$ ,  $1^4\Sigma^-$ ,  $1^4\Pi$ , and  $1^4\Delta$  lie between 0 and 0.6 eV. The  $2^4\Pi$  state, with a minimum slightly below 2.0 eV at  $R = 2.92 a_0$ , exhibits a second minimum ( $R_e = 4.46 a_0$ ,  $T_e = 2.14$  eV) due to an avoided crossing between the  $\text{Co}^+$  occupations  $d^8$  and  $d^7s$ . Such an interaction is also responsible for the shallow minima predicted for the  $2^4\Delta$  and  $2^4\Phi$  states. Several doublet states of  $\Sigma^-$ ,  $\Pi$ ,  $\Delta$ ,  $\Phi$ , and  $\Gamma$  character are bound. Except for  $1^2\Delta$ , they are expected to exhibit potential barriers along the dissociation path. All bound states have a  $d^7\sigma^2$  configuration ( $7\sigma$  is  $\text{CoH}$  bonding), with the exception of  $1^2\Delta$  which is  $d^8$ -like and has a significant  $d\sigma(\text{Co})$  contribution into the metal-hydrogen bond. The sextet states  $1^6\Delta$ ,  $1^6\Pi$ ,  $1^6\Sigma^-$ , and  $1^6\Phi$  are repulsive due to single occupation of  $7\sigma$ . The dissociation energy  $D_e(X^4\Phi)$  of 2.18 eV is in good agreement with experimental estimates. The ionization potential (IP) from  $X^3\Phi(\text{CoH})$  into  $X^4\Phi(\text{CoH}^+)$  ( $6\sigma \rightarrow \infty$ ) is calculated to be 7.23 eV, supporting an experimental lower limit of  $7.30 \pm 0.10$  eV for this quantity. The next IPs result from ionization of  $3\pi$  into  $1^4\Delta$  of  $\text{CoH}^+$  and  $1\delta$  into  $2^4\Pi$ , whereas  $7\sigma$  ionization is expected to break the  $\text{CoH}$  bond.

## I. INTRODUCTION

In recent years, considerable interest was shown in the gas phase chemistry of transition metal ions.<sup>1</sup> Experiments provided the thermodynamic data for a large number of organometallic compounds<sup>1</sup> as well as for positive ions of transition metal hydrides  $\text{MeH}^+$ .<sup>2</sup>

Dissociation energies have been measured for all  $\text{MeH}^+$  systems of the first transition series.<sup>2</sup> Gas phase reactions of  $\text{FeD}^+$  ( $\text{FeH}^+$ ),  $\text{CoD}^+$ , and  $\text{NiD}^+$  with hydrocarbons have also been studied.<sup>3</sup> Recently, reactions of  $\text{Co}^+$ ,  $\text{Ni}^+$ , and  $\text{Cu}^+$  with  $\text{H}_2$ ,  $\text{HD}$ , and  $\text{D}_2$  were examined using guided ion beam tandem mass spectrometry.<sup>4</sup> The ground electronic states of all three  $\text{Me}^+$  species were found to react efficiently above their thermodynamic thresholds, whereas excited  $\text{Me}^+$  states produced by electron impact reacted very inefficiently. Elkind and Armentrout<sup>4</sup> concluded that the reactivity of the  $\text{Me}^+ + \text{H}_2$  reactions is not controlled by the state of the reactant  $\text{Me}^+$  (ground or excited state) but by its electron configuration. Despite the vast literature published in the last years, no experimental information is available, as far as we know, for excited states of  $\text{MeH}^+$  radicals.

A few theoretical studies on  $\text{MeH}^+$  species have been published recently. Preliminary multireference density-configuration interaction (MRD-CI) results for  $\text{TiH}^+$  and  $\text{VH}^+$  indicated that  $R_e(\text{MeH}^+) < R_e(\text{MeH})$  (both species in the ground state) for  $8\sigma$  ionization from the neutral ground state configurations  $1\delta^3\pi^7\sigma^2 8\sigma(X^4\Phi, \text{TiH})$  and  $1\delta^3\pi^2 7\sigma^2 8\sigma(X^5\Delta, \text{VH})$ . Obviously,  $8\sigma$  ionization does not change  $\Lambda$ , though the multiplicity is reduced by one unit. A

detailed analysis of the electronic structures of the lowest-lying dissociation channels of pairs of  $\text{MeH}$  and  $\text{MeH}^+$  radicals arising from neighboring  $\text{Me}(Z)$  and  $\text{Me}^+(Z+1)$  atomic species ( $Z \equiv$  atomic number) showed that a given  $\text{Me}(Z+1)\text{H}^+$  system shows a pattern of low-lying states quite different from that assigned to the corresponding neutral  $\text{Me}(Z)\text{H}$  radical with the same number of electrons. For instance,  $\text{TiH}^+$  has a  $X^3\Phi$  ground state whereas  $\text{ScH}$  shows a  $X^1\Sigma^+$  ground state. Similarly,  $\text{VH}^+$  prefers a  $X^4\Delta$  ground state, which should be compared with  $X^4\Phi$  for neutral  $\text{TiH}$ . Differences in ground state structures between isovalent  $\text{Me}(Z+1)\text{H}^+$  and  $\text{Me}(Z)\text{H}$  species simply reflect the fact that  $\text{Me}^+(Z+1)$  and  $\text{Me}(Z)$  exhibit different ground states.<sup>5</sup> Alvarado-Swaisgood *et al.*<sup>6</sup> investigated three low-lying states of  $\text{ScH}^+$  as well as the ground state of  $\text{CrH}^+$ . Schilling *et al.*<sup>7</sup> reported calculations on the ground and selected excited states of all  $\text{MeH}^+$  systems from the first transition series. In the particular case of  $\text{CoH}^+$ , Schilling *et al.*<sup>7</sup> predicted the four lowest-lying quartet states to appear in the order  $X^4\Phi < 1^4\Sigma^- < 1^4\Pi < 1^4\Delta$ , and a low-lying  $1^2\Delta$  state was predicted at 0.76 eV, arising from the configuration  $1\delta^3 3\pi^4 7\sigma^2$  and showing a significantly shorter  $R_e$  than the above-mentioned quartet states. Petterson *et al.*<sup>8</sup> studied the spectroscopic parameters  $R_e$ ,  $\omega_e$  as well as dissociation energies and dipole moments for the complete series of  $\text{MeH}^+$  species, mainly in the ground states, from the first- and second-row transition metals. Both theoretical studies reported for  $\text{ScH}^+$ ,  $\text{TiH}^+$ , and  $\text{VH}^+$  similar dissociation energies and ground states as predicted by the MRD-CI computations.<sup>5</sup>

In the present communication, an extensive study on electronic states of  $\text{CoH}^+$  is reported, including states of doublet, quartet, and sextet multiplicity. Potential curves, spectroscopic parameters, electronic spectra, dissociation energies and ionization potentials will be discussed.

<sup>a)</sup> Present address: Departament de Química Física, Facultat de Química de Tarragona, Pl. Imperial Tàrraco, 43005 Tarragona, Spain.

<sup>b)</sup> Present address: Institute of Theoretical Chemistry, University of Bonn, Wegelerstrasse 12, 5300 Bonn 1, Germany.

<sup>c)</sup> Author to whom all correspondence should be sent.

## II. TECHNICAL DETAILS

Two basis sets were used to describe the transition metal. Basis set I starts with the 14s11p primitive set of Wachters,<sup>9</sup> contracted to 8s6p (contraction scheme number 3 of that work). The *d* set was taken from the study of Rappé *et al.*,<sup>10</sup> with 6*d* primitive functions contracted to 3*d*. Basis I also contains one *f* function ( $\alpha = 1.92$ ). Basis set II is built by adding a second, more compact *f* function ( $\alpha = 4.9$ ) to basis I. Both exponents have been optimized in this work by carrying out atomic calculations on the Co(<sup>4</sup>F, *d*<sup>7</sup>s<sup>2</sup>) atom. The H basis set is taken from Huzinaga,<sup>11</sup> consisting of 5s primitive Gaussians contracted to 2s, to which one semidiffuse *s* function ( $\alpha = 0.0202$ ) and a *p* ( $\alpha = 0.736$ ) and *d* ( $\alpha = 0.60$ ) polarization function were added. The molecular basis sets A and B are built by combining the H basis with the aforementioned basis sets I and II of Co, respectively.

All calculations were done by the MRD-CI method, which combines Table CI algorithms with configuration selection and extrapolation techniques.<sup>12,13</sup> Full CI (FCI) energies were estimated by generalizing the Langhoff and Davidson formula<sup>14,15</sup> to the multireference case. Estimated FCI energies will be given in the tables.

Only the outermost nine (ten) valence electrons of CoH<sup>+</sup> (CoH) were correlated since earlier experience with ScH, TiH, and VH<sup>5</sup> indicated that inclusion of 3s<sup>2</sup>3p<sup>6</sup> correlation does not significantly change the relative energies. A selection threshold of 4  $\mu$ hartree was used throughout. Potential curves were calculated from 2.2 to 5.0 *a*<sub>0</sub> by using basis set A and ground state MOs. The vertical spectrum was recalculated with basis B. Spectroscopic parameters were computed by the Dunham method.

## III. THE $X^3F(3d^8)$ AND $a^5F(3d^74s)$ STATES OF Co<sup>+</sup>

The ground and first-excited state of Co<sup>+</sup> were studied by correlating eight electrons and by using both basis sets I and II. The results are collected in Table I.

The SCF method erroneously predicts  $^5F(3d^74s)$  as the ground state, with errors in the relative stability of 1.76 eV (basis I) and 1.61 eV (basis II). Inclusion of electron correlation stabilizes the  $^3F$  state more than  $^5F$  (by about 1.40 eV), leading to an excitation energy of 0.20 eV in the best treatment. The experimental value is 0.44 eV.<sup>16</sup>

Schilling *et al.*<sup>7</sup> had some difficulties in describing the

relative separation  $\Delta E = E(^5F) - E(^3F)$ , as pointed out by CI values of  $-0.96$  or  $0.69$  eV, depending on the technical conditions of their calculations. On the other hand, Petterson *et al.*<sup>8</sup> obtained a nonrelativistic  $\Delta E$  of 0.33 eV by using an 8s6p4d 1*f* contracted set of Gaussian functions.

## IV. ELECTRONIC CONFIGURATIONS AND MOLECULAR ORBITALS

Table II shows experimental values of the first six dissociation channels of CoH<sup>+</sup> as well as the molecular states they correlate with. All possible configurations with up to three open shells resulting from the Co<sup>+</sup> atomic states  $3d^74s$  and  $3d^8$  are given in Table III, together with the corresponding doublet and quartet states of CoH<sup>+</sup>. Each configuration is labeled by a capital letter and a number, a notation used throughout this paper.

The first group, labeled *X*1, derives from the  $3d^74s$  atomic configuration. All molecular configurations in this group have  $7\sigma$ , which is mainly  $4s(\text{Co}^+) + 1s(\text{H})$ , doubly occupied, thereby describing bound states. The excitation  $7\sigma \rightarrow 8\sigma$  relative to the configurations *A*1 to *E*1 in Table III leads to configurations with five open shells giving rise to doublet, quartet and sextet states. These high-multiplicity states are referred to as *X*3, *X* being the same letter labeling the original configurations with  $7\sigma$  doubly occupied. All *X*3 states are expected to be repulsive since the  $\sigma$  bond is weakened. Such behavior has previously been predicted for the states of highest multiplicity of ScH, TiH, VH, and their corresponding positive ions for which  $7\sigma$  is singly occupied.<sup>5,17</sup>

The second group of configurations, labeled *X*2, results from  $3d^8$  atomic states. Except for *F*'2 and *G*'2, configurations from groups *X*1 and *X*2 having the same letter *X* generate exactly the same symmetry species and multiplicities. One notes that the pairs of configurations (*A*1, *A*2), (*D*1, *D*2) and (*E*1, *E*2) are related by the excitation  $7\sigma \rightarrow 6\sigma$  ( $4s \rightarrow 3d\sigma$ ), whereas *B*1 and *C*1 do not have counterparts in group 2. Similarly, the configurations in each of the pairs (*F*1, *F*2) and (*G*1, *G*2) are connected by the excitation  $7\sigma^2 \rightarrow 6\sigma^2$ . As shown below, both *F*2 and *G*2 configurations show a strongly bonding character due to  $3d\sigma + 4s$  hybridization and hydrogen admixture in the doubly occupied  $6\sigma$  MO. By contrast, the three open-shell configurations *F*'2

TABLE I. Calculated energies *E* (in hartree) and transition energies  $\Delta E$  (in eV) for the  $X^3F(3d^8)$  and  $a^5F(3d^74s)$  states of Co<sup>+</sup>. The experimental value of the transition energy is 0.44 eV.<sup>a</sup>

Method		Basis I (1 <i>f</i> )		Basis II (2 <i>f</i> )	
		$X^3F$	$a^5F$	$X^3F$	$a^5F$
SCF	<i>E</i> <sup>b</sup>	-0.8852	-0.9338	-0.9064	-0.9495
	$\Delta E$	0.00	-1.32	0.00	-1.17
MRD-CI	<i>E</i> <sup>b</sup>	-1.0812	-1.0778	-1.1217	-1.1145
	$\Delta E$	0.00	0.09	0.00	0.20

<sup>a</sup> Averaged over *M*<sub>J</sub> from Ref. 16.

<sup>b</sup> Relative to  $-1380.00$  hartree.

TABLE II. Correlation between atomic and molecular electronic states for the lower dissociation channels of CoH<sup>+</sup>.

Channel	$\Delta E$ (eV) <sup>a</sup>	Atomic state <sup>b</sup>	Molecular states
	(expt.)	Co <sup>+</sup>	CoH <sup>+</sup>
I	0.00	$X^3F(3d^8)$	$2^4(\Sigma^-, \Pi, \Delta, \Phi)$
II	0.44	$a^5F(3d^7[4F]4s)$	$4^6(\Sigma^-, \Pi, \Delta, \Phi)$
III	1.21	$^3F(3d^7[4F]4s)$	$2^4(\Sigma^-, \Pi, \Delta, \Phi)$
IV	1.56	$^3P(3d^8)$	$2^4(\Sigma^-, \Pi)$
V	1.92	$^5P(3d^7[4P]4s)$	$4^6(\Sigma^-, \Pi)$
VI	2.69	$^3P(3d^3[2P]4s)$	$2^4(\Sigma^-, \Pi)$

<sup>a</sup> Averaged *M*<sub>J</sub> values from Ref. 16.

<sup>b</sup> The coupling for *d*<sup>7</sup> is given in brackets.

TABLE III. Molecular configurations resulting from  $3d^7 4s$  and  $3d^8$  atomic configurations.

Atomic configuration	Notation	Molecular configuration	Molecular states
$\text{Co}^+ (3d^7 4s) + \text{H}(1s)$	A 1	$1\delta^3 3\pi^3 6\sigma 7\sigma^2$	$^2\Pi(2), ^2\Phi(2), ^4\Pi, ^4\Phi$
	B 1	$1\delta^3 3\pi^3 6\sigma^2 7\sigma^2$	$^2\Pi(2), ^2\Phi, ^2H, ^4\Pi$
	C 1	$1\delta^3 3\pi^2 6\sigma^2 7\sigma^2$	$^2\Sigma^+, ^2\Sigma^-, ^2\Delta(2), ^2\Gamma, ^4\Delta$
	D 1	$1\delta^3 3\pi^2 6\sigma 7\sigma^2$	$^2\Sigma^+, ^2\Sigma^-, ^2\Gamma, ^4\Sigma^-$
	E 1	$1\delta^4 3\pi^2 6\sigma 7\sigma^2$	$^2\Sigma^+, ^2\Sigma^-, ^2\Delta, ^4\Sigma^-$
	F 1	$1\delta^4 3\pi^3 7\sigma^2$	$^2\Pi$
	G 1	$1\delta^3 3\pi^4 7\sigma^2$	$^2\Delta$
	H 1	$1\delta^3 3\pi^4 6\sigma^2 7\sigma^2$	$^2\Delta$
	I 1	$1\delta^4 3\pi 6\sigma^2 7\sigma^2$	$^2\Pi$
	A 2	$1\delta^3 3\pi^3 6\sigma^2 7\sigma$	$^2\Pi(2), ^2\Phi(2), ^4\Pi, ^4\Phi$
	D 2	$1\delta^3 3\pi^4 6\sigma^2 7\sigma$	$^2\Sigma^+, ^2\Sigma^-, ^2\Gamma, ^4\Sigma^-$
$\text{Co}^+ (3d^8) + \text{H}(1s)$	E 2	$1\delta^4 3\pi^2 6\sigma^2 7\sigma$	$^2\Sigma^+, ^2\Sigma^-, ^2\Delta, ^4\Sigma^-$
	F 2 <sup>a</sup>	$1\delta^4 3\pi^3 6\sigma^2$	$^2\Pi$
	F' 2	$1\delta^4 3\pi^3 6\sigma 7\sigma$	$^2\Pi(2), ^4\Pi$
	G 2 <sup>a</sup>	$1\delta^3 3\pi^4 6\sigma^2$	$^2\Delta$
	G' 2	$1\delta^3 3\pi^4 6\sigma 7\sigma$	$^2\Delta(2), ^4\Delta$
	J	$1\delta^4 3\pi^4 7\sigma$	$^2\Sigma^+$

<sup>a</sup> For these configurations,  $6\sigma$  corresponds to a 50%–50% mixture between  $3d\sigma$  (Co) and  $1s$  (H).

and  $G'2$  (related to  $F2$  and  $G2$  by a  $6\sigma \rightarrow 7\sigma$  excitation) are expected to be repulsive.  $F'2$  and  $G'2$  give rise to doublet and quartet states of  $\Pi$  and  $\Delta$  symmetry, thereby taking the role of the “missed”  $B2$  and  $C2$  configurations mentioned above.

All configurations from group 1 use  $4s$  metal–hydrogen bonding by combining  $4s(\text{Co}^+)$  with  $1s(\text{H})$  to form  $7\sigma$  which is doubly occupied. By contrast, the formation of a Co–H bond is more limited in the case of group 2 ( $3d^8$  of  $\text{Co}^+$ ). The atomic occupation  $3d^7 d\sigma$  can generate the high-multiplicity repulsive configuration  $3d^7 6\sigma 7\sigma$  ( $F'2$ ,  $G'2$ ), where  $6\sigma$  is the atomic  $d\sigma$ , or the low-multiplicity (bound) configuration  $3d^7 6\sigma^2$  ( $F2$ ,  $G2$ ), where  $6\sigma$  results from pairing of  $1s(\text{H})$  with  $d\sigma$  of  $\text{Co}^+$ , leading to shorter equilibrium distances than those resulting from configurations of group 1. The analogy between the configurations  $d^7 6\sigma 7\sigma$  and  $d^7 6\sigma^2$  of  $\text{CoH}^+$  with the pairs  $d^n - ^1 6\sigma 7\sigma^2 8\sigma$  and  $d^n - ^1 6\sigma^2 7\sigma^2$  of neutral MeH species is worth mentioning. In both cases the low-multiplicity configurations show a significant  $d\sigma$  contribution to the bonding.

The orbital energies of the  $\text{Co}^+$  states  $^3F(3d^8)$  and  $^5F(3d^7 4s)$  and of the  $\text{CoH}^+$  states  $1^2\Delta(1\delta^3 3\pi^4 6\sigma^2)$  and

$1^4\Delta(1\delta^3 3\pi^2 6\sigma^2 7\sigma^2)$  are displayed in Table IV. It is seen that the orbital energies of  $1^4\Delta(\text{CoH}^+)$  are very similar to those of the  $^5F(3d^7 4s)$  state of  $\text{Co}^+$ . The same behavior is found for the corresponding MOs of  $X^4\Phi$ ,  $1^4\Sigma^-$ , and  $1^4\Pi$ , for example. These findings agree with the results from Ref. 7 about a  $d^7$ -like character for the lowest-lying quartet states of  $\text{CoH}^+$ . In general, the ground states of all  $\text{MeH}^+$  from the first transition metal series are predominantly of  $3d^7 4s$  character,<sup>7,8</sup> an observation probably valid for the corresponding low-lying excited states too.

For  $1^4\Delta$  the  $6\sigma$  MO is practically the atomic  $3d\sigma$ , while the bonding orbital  $7\sigma$  is mainly described by  $1s(\text{H})$  and  $4s(\text{Co}^+)$ , with minor contributions from  $4p\sigma$  and  $3d\sigma$  of  $\text{Co}^+$ .<sup>7,8</sup> A pictorial representation of the natural orbitals  $6\sigma$  and  $7\sigma$  of  $X^4\Phi$  is given in Ref. 8.

## V. POTENTIAL CURVES

### A. Quartet $\Pi$ and $\Phi$ states

Vertical excitation energies and electronic configurations at 2.9 to 3  $a_0$  are collected in Table V. Potential curves

TABLE IV. Orbital energies (in hartree) for valence orbitals of  $X^3F$  and  $a^5F$  states of  $\text{Co}^+$  and  $^2\Delta$  ( $G1$ ) and  $1^4\Delta$  ( $C1$ )<sup>a</sup> states of  $\text{CoH}^+$ .

$\text{Co}^+ (X^3F, 3d^8)$	$\text{Co}^+ (a^5F, 3d^7 4s)$	$\text{CoH}^+ (^2\Delta)$ ( $R = 3.0 a_0$ )	$\text{CoH}^+ (1^4\Delta)$ ( $R = 3.0 a_0$ )
$3s - 4.6159$	$3s - 4.8483$	$4\sigma - 4.8126$	$4\sigma - 4.8588$
$3p - 3.1159$	$3p - 3.3320$	$5\sigma - 3.3029$	$5\sigma - 3.3431$
		$2\pi - 3.2986$	$2\pi - 3.3419$
$3d - 0.7475$	$3d - 0.9857$	$3\pi - 0.9119$	$3\pi - 1.0429$
		$1\delta - 0.8796$	$1\delta - 0.9954$
			$6\sigma - 0.9506$
	$4s - 0.5760$	$7\sigma - 0.6653$	$7\sigma - 0.6458$
$1s(\text{H}) - 0.4998$			

<sup>a</sup> See Table III.

TABLE V. Calculated adiabatic excitation energies  $T_e$  for doublet and quartet states of CoH<sup>+</sup>. (All values are estimated full CI energies.)<sup>a</sup>

State	Configuration <sup>b</sup>	$T_e$ (eV)
$X^4\Phi$	$A1$	0.00
$1^4\Sigma^-$	$D1-E1$	0.08
$1^4\Pi$	$A1(B1)$	0.28
$1^4\Delta$	$C1$	0.58
$1^2\Delta$	$G2(G'2)$	1.18
$1^2\Phi$	$A1(A2)$	1.61
$2^4\Sigma^-$	$D1+E1$	1.65
$1^2\Pi$	$A1(A2F2)$	1.70
$1^2\Sigma^-$	$D1-E1(D2E2)$	1.88
$2^4\Pi$	$B1(A1)$	1.92
	$A2(A1)$	2.14 <sup>c</sup>
$2^4\Phi$	$A2(A1)$	2.18
$2^4\Delta$	$G'2(C1)$	2.20
$2^2\Pi$	$A1(A2)$	2.35
$1^2\Gamma$	$D1(C1)$	2.64
$2^2\Delta$	$C1$	3.08

<sup>a</sup>The total energies for  $X^4\Phi$  are -1381.6659 hartree, basis A, and -1381.7018 hartree, basis B.  $T_e$  values from basis A.

<sup>b</sup>See Table III.

<sup>c</sup>Right minimum at 4.46  $a_0$ .

for  $4^4\Pi$  and  $4^4\Phi$  states are shown in Fig. 1. In this and similar figures, the atomic separations correspond to experimental values.<sup>16</sup>

According to the discussion from Sec. IV, the two  $4^4\Pi$  states of  $d^7s$  character (configurations  $A1$  and  $B1$ ) should lead to bound states of CoH<sup>+</sup>. By contrast, both  $d^8$ -like  $4^4\Pi$  states ( $A2$  and  $F'2$ ) are unable to form a Co-H bond and should exhibit repulsive behavior. Since two  $4^4\Pi$  states are repulsive but the other two are bound, avoided crossings are expected between them. The two  $4^4\Phi$  states result from  $A1$  and  $A2$ , and again a crossing is expected between them due to

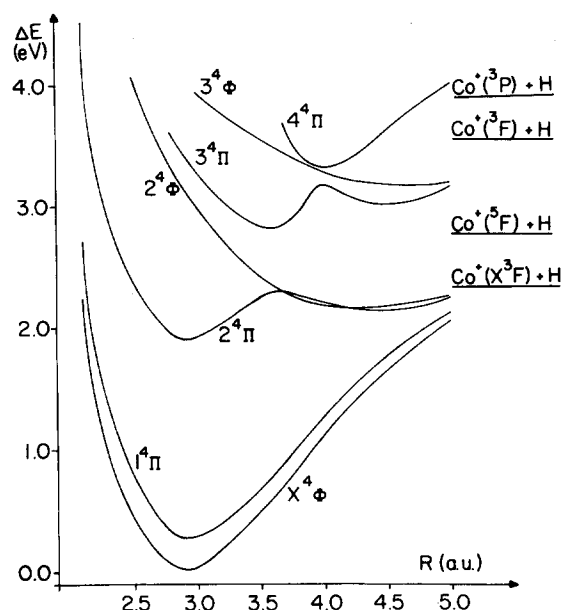


FIG. 1. Calculated potential energy curves (basis A and FCI results) for various quartet  $\Phi$  and  $\Pi$  states of CoH<sup>+</sup>. The lowest dissociation limits are also given.

the bonding and antibonding character of  $A1$  and  $A2$ , respectively.

The potential curves shown in Fig. 1 are in full agreement with these expectations. From the four  $4^4\Pi$  states and three  $4^4\Phi$  studied in this work, only  $X^4\Phi(A1)$ ,  $1^4\Pi(A1, B1)$  and  $2^4\Pi(B1)$  show minima at equilibrium distances near 3.0  $a_0$ .

The  $2^4\Phi$  state exhibits a shallow minimum around 4.3  $a_0$ . It arises from the avoided crossing between  $A1$  (bonding) and  $A2$  (repulsive). The  $3^4\Phi$  state is repulsive in the whole range of nuclear distances investigated, in agreement with its leading configuration  $A3$ , having all  $\sigma$  MOs singly occupied.

The  $1^4\Pi$  state lies about 0.3 eV above  $X^4\Phi$ . Both states derive from the configuration  $A1$  and show similar potential curves.  $1^4\Pi$  also has some contribution from  $B1$  ( $\sim 25\%$ ), as expected from the asymptotic description of  $4^4\Pi(d^7s, ^3F)$ . Around  $R = 3.0 a_0$ ,  $2^4\Pi$  is mainly described by  $B1$  with some admixture of  $A1$ . The flat minimum around 4.5  $a_0$  results from an avoided crossing between  $2^4\Pi(A2)$  and  $1^4\Pi(A1, B1)$ , similar to the interaction between  $2^4\Phi(A2)$  and  $X^4\Phi(A1)$ .

The heavy mixing between 2, 3, and  $4^4\Pi$  is shown in Fig. 2, where the contributions (in terms of  $c^2$ ) of the most relevant configurations are plotted as a function of  $R$ . For instance,  $B1$  characterizes  $2^4\Pi$  at shorter  $R$ ,  $3^4\Pi$  around 4.0  $a_0$  and  $4^4\Pi$  at larger  $R$ .  $A2$  characterizes  $2^4\Pi$  from 4.0 to 5.0  $a_0$  and  $3^4\Pi$  at shorter  $R$ , whereas the repulsive configura-

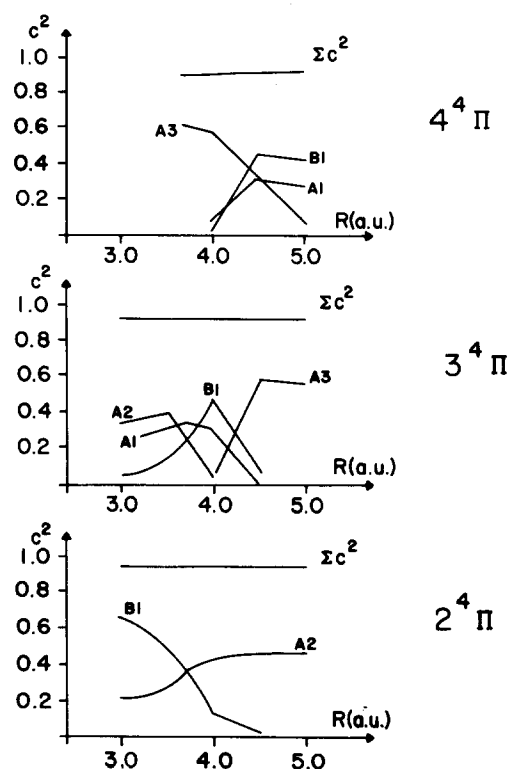


FIG. 2. Contribution ( $c^2$ ) to the wave function of the most important configurations describing  $2^4\Pi$ ,  $3^4\Pi$ , and  $4^4\Pi$  states. The configurations are  $A1(1d^33\pi^36\sigma^7\sigma^2)$ ,  $A2(1d^33\pi^36\sigma^7\sigma)$ ,  $A3(1d^33\pi^36\sigma^7\sigma^2\sigma)$ , and  $B1(1d^33\pi^36\sigma^7\sigma^2)$ .

tion  $A\ 3$  describes  $3\ ^4\Pi$  at larger  $R$  but  $4\ ^4\Pi$  at shorter distances.

### B. Quartet states of $\Sigma^-$ and $\Delta$ symmetry

Potential curves for  $^4\Sigma^-$  and  $^4\Delta$  states are displayed in Fig. 3. Of the four  $^4\Sigma^-$  states listed in Table III, two result from  $3d\ 7s$  atomic configurations ( $D\ 1$  and  $E\ 1$ ) and are expected to be bonding. The other two result from  $3d\ ^8$  ( $D\ 2$  and  $E\ 2$ ), and are expected to be repulsive, showing avoided crossings with the bound states.

$1\ ^4\Sigma^-$  and  $2\ ^4\Sigma^-$  are described at equilibrium by  $d\ ^7$ -like configurations, with  $D\ 1$  predominating in  $1\ ^4\Sigma^-$  and  $E\ 1$  mainly describing  $2\ ^4\Sigma^-$ . The  $2\ ^4\Sigma^-$  potential curve changes its curvature around  $4\ a_0$  due to an avoided crossing with  $3\ ^4\Sigma^-$ . Energetically,  $1\ ^4\Sigma^-$  lies slightly above  $X\ ^4\Phi$  while  $2\ ^4\Sigma^-$  is similar in energy to  $2\ ^4\Pi$ , the latter two states correlating diabatically with  $\text{Co}^+ (^5P) + \text{H}$ .

The interaction between  $2\ ^4\Sigma^-$ ,  $3\ ^4\Sigma^-$ , and  $4\ ^4\Sigma^-$  is represented in Fig. 4 by plotting the contributions of several configurations to the respective wavefunctions. One notes that  $D\ 1$  and  $E\ 1$  characterize  $2\ ^4\Sigma^-$  at shorter  $R$ ,  $3\ ^4\Sigma^-$  around  $4\ a_0$  and  $4\ ^4\Sigma^-$  at larger  $R$ . The configurations  $D\ 3$  and  $E\ 3$ , with five open shells, describe  $4\ ^4\Sigma^-$  at shorter  $R$  and  $3\ ^4\Sigma^-$  at larger  $R$ , while  $D\ 2$  and  $E\ 2$  are the leading configurations of  $3\ ^4\Sigma^-$  at shorter  $R$  and  $2\ ^4\Sigma^-$  up to  $3.5\ a_0$ . As seen in Fig. 3, the  $3\ ^4\Sigma^-$  potential curve is highly anharmonic, an observation also valid for the  $3\ ^4\Pi$  state (Fig. 1).

As shown in Table V, at equilibrium  $1\ ^4\Delta$  arises from  $C\ 1$  whereas the  $2\ ^4\Delta$  state has predominantly  $G\ ^2$  character. Since  $1\ ^4\Delta$  dissociates to  $\text{Co}^+ (3d\ 7s) + \text{H}$ , whereas  $2\ ^4\Delta$  dissociates to the lower-lying  $\text{Co}^+ (3d\ ^8)$  (Table II), an avoided crossing occurs, giving  $2\ ^4\Delta$  a shallow minimum around  $4\ a_0$  (lying about 0.5 eV below channel II).

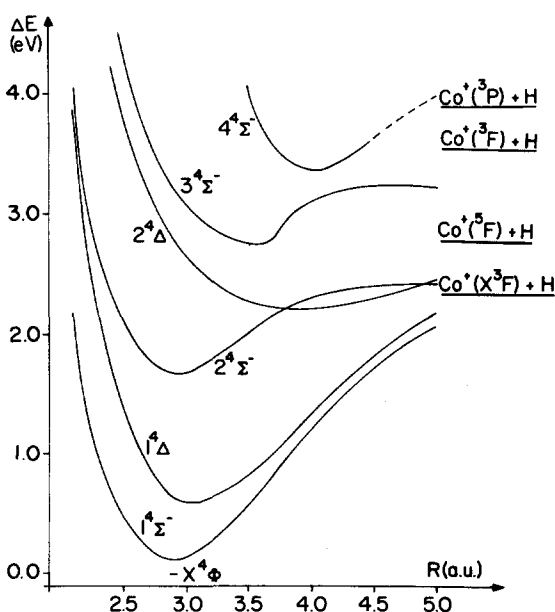


FIG. 3. Calculated potential energy curves (basis A and FCI results) for various quartet  $\Delta$  and  $\Sigma^-$  states of  $\text{CoH}^+$ . The lowest dissociation limits are also given.

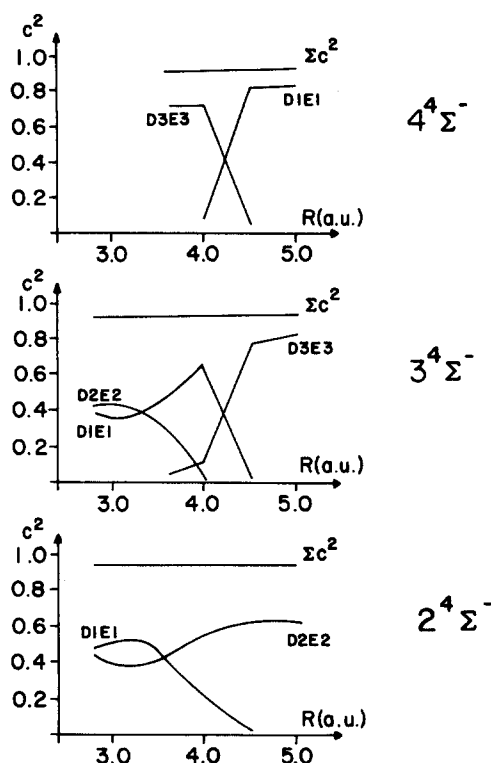


FIG. 4. Contribution ( $c^2$ ) to the wave function of the most important configurations describing  $2\ ^4\Sigma^-$ ,  $3\ ^4\Sigma^-$ , and  $4\ ^4\Sigma^-$  states. The configurations are  $D\ 1(1d^23\pi^6\sigma^7\sigma^2)$ ,  $E\ 1(1d^43\pi^2\sigma^7\sigma^2)$ ,  $D\ 2(1d^23\pi^4\sigma^7\sigma^2)$ ,  $E\ 2(1d^43\pi^2\sigma^7\sigma^2)$ ,  $D\ 3(1d^23\pi^4\sigma^7\sigma^8\sigma)$ , and  $E\ 3(1d^43\pi^2\sigma^7\sigma^8\sigma)$ .

### C. Doublet states

The potential curves of several doublet states are shown in Fig. 5. By comparing Figs. 1, 3, and 5 it is easily seen that the quartet-doublet separations among pairs of states arising

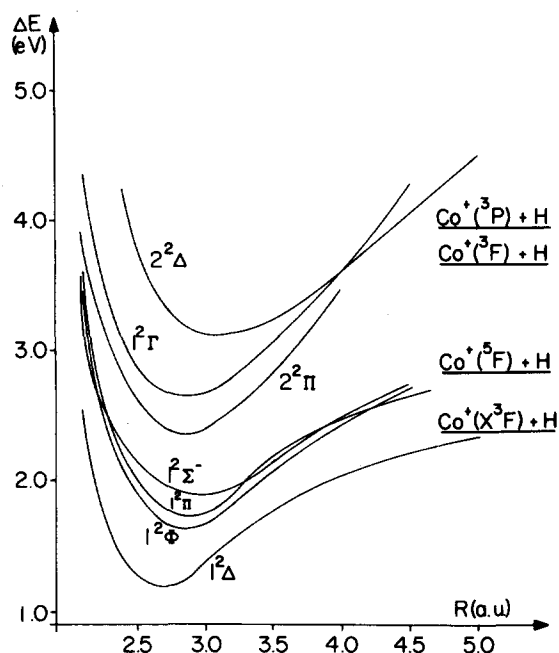


FIG. 5. Calculated potential energy curves (basis A and FCI results) for doublet states of  $\text{CoH}^+$ . The lowest dissociation limits are also given.

from a common configuration are quite large, above 1.5 eV. For comparison, the multiplet separations in neutral species such as ScH, TiH, and VH<sup>5,17</sup> are smaller (well below 1.0 eV).

As indicated in Table II, both the first ( $d^8$ ) and the third ( $d^7$ ) dissociation limits give rise to doublets of symmetry  $\Sigma^-$ ,  $\Pi$ ,  $\Delta$ , and  $\Phi$ . Except for  $F2$  and  $G2$ , however, the  $d^8$  configurations from channel I generate repulsive doublet states for the same reasons as discussed in Sec. V for quartet states. Similarly, channel III only generates repulsive doublets of the type  $X3(d^7\sigma^2)$  because of its intrinsic  $^4F(d^7)$  coupling. Bound doublet states with configuration  $d^7\sigma^2$  correlate (in a diabatic sense) with those  $d^7s$  states of  $\text{Co}^+$  which have an intrinsic  $^2X(d^7)$  coupling.

Reference 16 places the  $\text{Co}^+$  states  $^3P(d^7[^2P]s)$  and  $^3D(d^7[^2D]s)$  at 3.09 and 3.47 eV, respectively. The atomic configuration  $d^7s$  also generates  $^2F$ ,  $^2G$ , and  $^2H$ , but these states have not been observed<sup>16</sup> and are expected to be less stable. Taking channel III as reference (an asymptote limit leading to doublet states but with  $^4F(d^7)$  coupling), the aforementioned  $^3P$  state lies 1.88 eV higher. This simple analysis already points to a relatively large quartet-doublet splitting for the atomic  $d^7$  species, a feature which is transferred to the  $\text{CoH}^+$  radical as demonstrated by the present results.

According to the information contained in Table V and Fig. 5,  $1^2\Phi$ ,  $1^2\Pi$ , and  $1^2\Sigma^-$  show minima in the expected energy region (i.e., approximately 1.7 eV above the quartet states), whereas  $1^2\Delta$  is more stable by about 0.60 eV. Differences in equilibrium stabilities between  $1^2\Delta$  and the other three doublet states can be understood since  $1^2\Delta$  is a  $d^8$  state (like its dissociation limit), whereas  $1^2\Phi$ ,  $1^2\Pi$ , and  $1^2\Sigma^-$  are mainly of  $d^7$  character (higher channels), with some contribution from  $d^8$  configurations.

As mentioned before,  $1^2\Phi$ ,  $1^2\Pi$ , and  $1^2\Sigma^-$  represent in essence the doublet counterparts of the  $d^7$  states  $X^4\Phi$ ,  $1^4\Pi$ , and  $1^4\Sigma^-$ , respectively. At equilibrium, these doublet states lie about 0.50 eV below their dissociation limit, whereas near  $4.5 a_0$  they are about 0.30 eV above it, a feature obviously indicating the existence of potential barriers for  $R > 4.5 a_0$  (Fig. 5).

The higher-lying states  $2^2\Pi$  and  $2^2\Delta$  correlate (adiabatically) with channel III. Near equilibrium,  $2^2\Pi$  contains contributions from both  $A1$  and  $A2$ , while  $2^2\Delta$  arises from  $C1$ . Both states are separated by about 2.5 eV and show minima around  $3.0 a_0$  (Figs. 3 and 5). As  $R$  increases,  $2^2\Delta$  acquires  $G2$  character as a result of an interaction with  $1^2\Delta$ .

The  $1^2\Gamma$  state dissociates into products of the type  $\text{Co}^+ (^1G) + \text{H}$ . The exact nature of its dissociation limit remains unclear since the atomic states  $^1G(d^8)$  and  $^1G(d^7s)$  have not been experimentally observed (at least in the compilation from Ref. 16). Only a multiplet  $^3G(d^7p)$  is known for  $\text{Co}^+$ .

As seen in Fig. 5, the potential curves of  $2^2\Pi$  and particularly of  $2^2\Delta$  do not show any tendency to correlate with channel III. This indicates the existence of substantial potential barriers along the dissociation path, much higher than

those expected for the states  $1^2\Phi$ ,  $1^2\Pi$ , and  $1^2\Sigma^-$ . However, since such barriers result from a switch between configurations of  $d^7$  type having different intrinsic couplings, it is quite probable that spin-orbit effects are relevant in the description of the doublet potential curves at intermediate and larger distances, making the "true" potential curves not as steep as suggested by Fig. 5.

#### D. Sextet states

The four sextet states correlating with channel II have been studied only at  $R = 3 a_0$ . They are described by the repulsive  $X3(d^7 \text{ like})$  configurations discussed in Sec. IV.

At  $R = 3.0 a_0$ , their energetic positions (in eV) are 3.61 for  $1^6\Delta(1\delta^3\pi^26\sigma^27\sigma^2)$ , 3.83 for  $1^6\Pi(1\delta^3\pi^36\sigma^27\sigma^2)$ , 4.29 for  $1^6\Sigma^-$  (mixture between  $1\delta^3\pi^46\sigma^27\sigma^2$  and  $1\delta^4\pi^26\sigma^27\sigma^2$ ) and 4.33 for  $1^6\Phi(1\delta^3\pi^36\sigma^27\sigma^2)$ . Combining the dissociation energy of  $X^4\Phi$  with the  $\text{Co}^+$  excitation energy between  $^3F(3d^8)$  and  $^5F(3d^74s)$ , channel II is placed 2.62 eV above  $X^4\Phi$  at equilibrium. Hence, at  $R = 3a_0$  these sextet states are from 1.0 to 1.70 eV less stable than their dissociation limit.

The sextet states  $2^6\Sigma^-$  and  $2^6\Pi$  correlating with channel V (Table II) have not been studied. They are expected to be repulsive and to lie about 1.50 eV above  $1^6\Sigma^-$  and  $1^6\Pi$  (same separation as between the atomic states  $^5F$  and  $^5P(3d^74s)$ , Table II).

#### VI. EXCITATION ENERGIES AND SPECTROSCOPIC PARAMETERS

Excitation energies  $T_e$  and spectroscopic data of 16 low-lying bound states are collected in Tables V and VI, respectively.

Though the inclusion of a second, more compact  $f$  function lowers the total energy of  $X^4\Phi$  by about 1.0 eV (a value comparable to the stabilization of the atomic states in going from basis I to basis II, Table I), around  $R_e$  the extension of the basis set has only a minor effect on the relative stabilities.

The states  $X^4\Phi$ ,  $1^4\Sigma^-$ ,  $1^4\Pi$ , and  $1^4\Delta$ , all having  $d^7$  character, lie within the 0.0 to 0.6 eV energy region. The present MRD-CI results confirm the ordering of states and the excitation energies predicted by Schilling *et al.*,<sup>7</sup> though the total energies reported by these authors are about 1.4 hartree higher.

Since the neutral radical FeH (isovalent with  $\text{CoH}^+$ ) shows a  $X^4\Delta(1\delta^3\pi^26\sigma^27\sigma^2)$  ground state and a low-lying  $1^6\Delta(1\delta^3\pi^26\sigma^27\sigma^2)$  state,<sup>8</sup> one has another example of the dissimilarities between neighboring MeH and MeH<sup>+</sup> species with respect to the character of their corresponding ground and low-lying states as mentioned in the Introduction (see also Ref. 5). However, since the first excited state of Fe,  $^5F(3d^74s)$ , corresponds exactly to that of  $\text{Co}^+$  (Table II) and the four lowest-lying quartet states of  $\text{CoH}^+$  correlate diabatically with this channel, the second channel states of FeH are expected to resemble (in structure and in their relative position) the features predicted here for  $\text{CoH}^+$ .

As shown in Table VI, the present study indicates that  $R_e(X^4\Phi) \approx R_e(1^4\Sigma^-) < R_e(1^4\Pi) < R_e(1^4\Delta)$ . A similar

TABLE VI. Calculated spectroscopic parameters for the low-lying electronic states of CoH<sup>+</sup>.

State	$R_e (a_0)$	$\omega_e (\text{cm}^{-1})$	$\omega_e x_e (\text{cm}^{-1})$	$B_e (\text{cm}^{-1})$	$\alpha_e (\text{cm}^{-1})$
$X^4\Phi$	2.90	2025	43.6	7.22	0.22
Ref. 7	3.03	1631			
Ref. 8	2.92	1888			
$1^4\Sigma^-$	2.90	2007	41.9	7.22	0.22
Ref. 7	3.03	1619			
$1^4\Pi$	2.95	1940	44.4	6.98	0.21
Ref. 7	3.05	1631			
$1^4\Delta$	3.06	1820	45.9	6.49	0.25
Ref. 7	3.21	1616			
$1^2\Delta$	2.73	2092	69.2	8.19	0.28
Ref. 7	2.76	1992			
$1^2\Phi$	2.85	1960	56.4	7.48	0.27
$2^4\Sigma^-$	2.93	1920			
$1^2\Pi$	2.88	2010	76.1	7.76	0.29
$1^2\Sigma^-$	2.97	1590	63.2	7.33	0.31
$2^4\Pi^a$	2.92	1930	81.4	7.13	0.17
$2^4\Pi^b$	4.46	860			
$2^4\Phi$	4.27	745			
$2^4\Delta$	3.91	770			
$2^2\Pi$	2.85	1952	54.8	7.50	0.17
$1^2\Gamma$	2.86	1912	44.5	7.50	0.20
$2^2\Delta$	3.05	1770	59.2	6.58	0.26

<sup>a</sup> Left minimum.<sup>b</sup> Right minimum.

behavior has been reported in Ref. 7, though their calculated  $R_e$ 's are larger than ours by about  $0.1 a_0$ . Accordingly, we assign to the lowest-lying quartet states higher  $\omega_e$ 's ( $\sim 150$  to  $400 \text{ cm}^{-1}$ ) than those predicted earlier. On the other hand, Petterson *et al.*<sup>8</sup> obtained for  $X^4\Phi$   $R_e = 2.923a_0$  (nonrelativistic result) and  $\omega_e = 1888 \text{ cm}^{-1}$ , both estimates lying close to the present results.

The energetic separations  $\Delta E (2^4\Sigma^- - 1^4\Sigma^-)$  of 1.57 eV and  $\Delta E (2^4\Pi - 1^4\Pi)$  of 1.64 eV compare well with a  $\Delta E$  of 1.79 eV between channels II and V (Table II). Though the equilibrium geometries and vibrational frequencies of these pairs of  $^4\Sigma^-$  and  $^4\Pi$  states are comparable, the avoided crossings affecting the higher-lying states  $2^4\Sigma^-$  and  $2^4\Pi$  are reflected in their large anharmonicity parameters  $\omega_e x_e$ .

## VII. ELECTRONIC SPECTRUM

Absorption from  $X^4\Phi$  into upper states of  $^4\Phi$ ,  $^4\Delta$ , and  $^4\Gamma$  character is possible.  $^4\Gamma$  states have not been studied here since, if stable at all, they should lie at much higher energies.

The transition  $1^4\Delta \leftarrow X^4\Phi$  occurs in the infrared region. Its intensity should be rather low since this band involves a  $3\pi \rightarrow 6\sigma$  ( $d \rightarrow d$ ) excitation. If detectable, some vibrational structure should be present due to differences in  $R_e$  and  $\omega_e$ .

The second transition,  $2^4\Delta \leftarrow X^4\Phi$ , lies in the visible region (from 2.20 to 2.89 eV, Fig. 3). At  $R = 2.9 a_0$ , this transition results from the excitation  $7\sigma \rightarrow 3\pi$ , that is, from the bonding  $7\sigma$  MO into the  $3d$  subshell. This absorption band should exhibit a rather complex structure since (1)  $R_e(2^4\Delta)$  is larger than  $R_e(X^4\Phi)$  by about  $1.0 a_0$ ; (2)  $1^4\Delta$  and  $2^4\Delta$  have an avoided crossing near  $4.0 a_0$ ; (3) at  $R = 3 a_0$ ,  $2^4\Delta$  lies  $\sim 0.4 \text{ eV}$  above the first dissociation limit (Fig.

3); and, (4) near its minimum,  $2^4\Delta$  is crossed by the states  $2^4\Sigma^-$ ,  $2^4\Pi$ , and  $2^4\Phi$  (Figs. 1 and 3). Altogether, this region of the spectrum is expected to contain a broad vibrational progression and quite certainly a dissociative continuum.

Since the  $2^4\Phi$  potential curve is similar to that of  $2^4\Delta$ , the transition  $2^4\Phi \leftarrow X^4\Phi$  ( $7\sigma \rightarrow 6\sigma$ ) should have a structure similar to that of  $2^4\Delta \leftarrow X^4\Phi$ , discussed above.

Good candidates for an emission spectrum are transitions from  $2^4\Sigma^-$  or  $2^4\Pi$  (inner minimum) into the states  $1^4\Sigma^-$  and/or  $1^4\Pi$ . These bands extend from 1.30 to 1.85 eV. On the other hand, emission from  $2^4\Delta$  or  $2^4\Phi$  into lower states with the appropriate symmetry are unlikely since both upper quartet states are energetically close to the first dissociation limit, and interact strongly with the nearby  $1^4\Delta$  and  $X^4\Phi$  states (at  $R \simeq 4.0 a_0$ ), respectively.

## VIII. DISSOCIATION ENERGIES

The dissociation energy ( $D_e$ ) of CoH<sup>+</sup> ( $X^4\Phi$ ), calculated with basis sets A and B, is given in Table VII together with experimental<sup>14,19,20</sup> and theoretical<sup>7,8</sup> results from the literature.

In going from basis A (1f) to basis B (2f), the  $D_e$  value of the ground state is lowered by 0.12 eV due to the better description of the  $d^8$  ground state of Co<sup>+</sup> in the larger basis set (Sec. III). Taking into account a zero-point energy of about 0.12 eV (Table VI), we obtain a  $D_0(X^4\Phi)$  of 2.06 eV, in reasonable agreement with experimental estimates of  $1.98 \pm 0.06 \text{ eV}$ ,<sup>4</sup>  $2.25 \pm 0.17 \text{ eV}$ <sup>20</sup> and  $2.10 \pm 0.09 \text{ eV}$ .<sup>21</sup> Earlier *ab initio* studies reported  $D_0$  values of 1.89 eV<sup>7</sup> and 1.77 eV (uncorrected) or 1.98 eV (corrected).<sup>8</sup> It is worth mentioning that  $D_0 = 1.98 \text{ eV}$  from Ref. 4 has been deduced



TABLE VII. Calculated dissociation energy  $D_e$  of  $\text{CoH}^+$ .<sup>a</sup> All values in eV.

Basis A		Basis B		Basis A		Basis B	
Channel I states			Channel II states				
$X^4\Phi$	2.30	2.18	$2^4\Sigma^-$	1.09	1.00		
$1^4\Sigma^-$	2.22	2.10	$2^4\Pi^b$	0.82	0.66		
$1^4\Pi$	2.02	1.84	$2^4\Delta$	0.54			
$1^4\Delta$	1.72	1.50	$2^4\Phi$	0.56			
$1^2\Delta$	1.12	1.02	Channel III states				
$1^2\Phi$	0.69	0.57	$2^2\Pi$	1.16			
$1^2\Pi$	0.60	0.49	$2^2\Delta$	0.43	0.19		
$1^2\Sigma^-$	0.42	0.32					

<sup>a</sup> For channels II and III, the experimental  $\Delta E$  of  $\text{Co}^+$  from Table II have been used.<sup>b</sup> Left minimum

by combining experimental data and phase space calculations, the latter using as input *ab initio* spectroscopic results from Schilling *et al.*<sup>7</sup> However, as stated in Sec. VI, the present study agrees with the study carried out by Petterson *et al.*<sup>8</sup> in assigning to the ground state of  $\text{CoH}^+$  a shorter  $R_e$  and a higher  $\omega_e$  than reported earlier.<sup>4,7</sup>

The bond strength of other electronic states can be derived straightforwardly by combining  $D_e(X^4\Phi)$  with the information contained in Tables II and V. The corresponding  $D_e$  values are also listed in Table VII.

The lowest-lying states  $1^4\Sigma^-$ ,  $1^4\Pi$ , and  $1^4\Delta$  exhibit similar  $D_e$  values of 1.50 to 2.10 eV due to their double occupation of the bonding MO  $7\sigma$  and the fact that crossings with  $d^8$ -like configurations take place at larger  $R$ . By contrast, the second channel states  $2^4\Sigma^-$ ,  $2^4\Pi$ ,  $2^4\Delta$ , and  $2^4\Phi$  are significantly less stable. The  $d^7$ -type states  $2^4\Sigma^-$  and  $2^4\Pi$  have “anomalous” dissociation energies because they correlate adiabatically with  $\text{Co}^+(d^7[4F]s) + \text{H}$  whereas at equilibrium  $2^4\Sigma^-$  and  $2^4\Pi$  have a  $^4P$  coupling for the  $d^7$  subshell (Sec. V). Along the dissociation path the potential curves of  $2^4\Sigma^-$  and  $2^4\Pi$  all are crossed twice, namely by  $d^8$  configurations around  $3.5 a_0$  and by a  $d^7$  configuration with a  $^4F$  coupling at  $R \geq 5.0 a_0$  (Figs. 1 and 2). On the other hand, the small dissociation energies of  $2^4\Delta$  and  $2^4\Phi$  reflect the mixed character  $d^8/d^7$  of both states at equilibrium.

$1^2\Delta$ , the only bound state with definite  $d^8$  character and  $d\sigma$  bonding, has a  $D_e$  of 1.12 eV (basis A) or 1.02 eV (basis B), a result which should be compared with  $D_e = 1.23$  eV predicted in Ref. 7.

The doublet states  $1^2\Phi$ ,  $1^2\Pi$ ,  $1^2\Sigma^-$ , and  $2^2\Delta$  exhibit smaller dissociation energies (from 0.20 to 0.60 eV), whereas  $2^2\Pi$  has  $D_e \approx 1.15$  eV. As discussed in Sec. V C, the potential curves of these doublet states show dissociation barriers due to significant differences in structure (i.e.,  $d^7$  vs  $d^8$  as well as doublet versus quartet coupling for the  $d$  subshell) between equilibrium and the corresponding dissociation limits. For these reasons, at equilibrium the aforementioned low-multiplicity states appear to be more strongly bound (as reflected by their short  $R_e$ 's and high  $\omega_e$ 's) than expected by their relatively small adiabatic dissociation energies.

## IX. IONIZATION POTENTIALS

Photoelectron spectroscopy (PES) is a valuable experimental technique for the characterization of positive ions. This is particularly important for  $\text{MeH}^+$  species since their low-lying states result from  $d^n 7\sigma^2$  configurations so that transitions between them, usually in the infrared region, have a rather weak intensity ( $d \rightarrow d$  type transition). Moreover, positive ions are in general less stable and more difficult to handle in spectroscopic studies, often making PES the only experimental technique applicable. Therefore, it is worthwhile to discuss the IPs of  $\text{CoH}$  in some detail. The predicted IPs are given in Table VIII.

The  $\text{CoH}$  radical has a  $X^3\Phi(1d^3 3\pi^3 6\sigma^2 7\sigma^2)$  ground state, with an experimental  $R_e$  close to  $2.91 a_0$ .<sup>18</sup> The first IP results from  $6\sigma$  ionization, leading to  $X^4\Phi$  and  $1^4\Pi$  of  $\text{CoH}^+$ . The ground state of the positive ion is predicted to be 7.23 eV (basis B) above the neutral state, a result supporting an experimental IP of  $7.3 \pm 0.1$  eV.<sup>20</sup> However, it should be mentioned that the experimental value does not correspond to a direct PES measurement but was derived by comparing fragmentation yields of  $\text{CoH}^+$  with respect to compounds with known IPs. In addition, the experimentalists considered their estimated IP( $\text{CoH}$ ) to be a lower limit (footnote 43 in Ref. 20). On the other hand, assuming an error of about  $-0.30$  eV for the present theoretical IPs,<sup>5</sup> the first IP( $\text{CoH}$ ) might lie close to 7.50 to 7.60 eV, that is, slightly smaller than the relative separation of 7.86 eV<sup>16</sup> between the ground states of  $\text{Co}(d^7s)$  and  $\text{Co}^+(d^8)$ .

The first ionization region should also contain a second peak since the  $1^4\Pi$  state is located about 0.30 eV above the  $X^3\Phi \rightarrow X^4\Phi$  line. No vibrational structure is expected for  $6\sigma$  ionization since the ionic states have  $R_e$  values (Table VI) close to  $R_e(X^3\Phi)$  of  $\text{CoH}$ , a feature corroborating the non-bonding nature of the  $6\sigma(3d\sigma)$  MO for these states.

The next IP, resulting from  $3\pi$  ionization and leading to  $1^4\Delta$ , is calculated to be 7.87 eV (or  $\approx 8.20$  eV corrected). This band might exhibit some vibrational structure since  $R_e(1^4\Delta)$  is larger than  $R_e(X^3\Phi)$  by about  $0.15 a_0$  (Table VIII) and the vibrational frequency is lowered by about  $100 \text{ cm}^{-1}$  with respect to  $\omega_e(X^3\Phi) = 1925 \text{ cm}^{-1}$ .<sup>18,21</sup>

TABLE VIII. Ionization potential IP for ionization of CoH ( $X^3\Phi$ ,  $1\delta^3 3\pi^3 6\sigma^2 7\sigma^2$ )<sup>a</sup> into quartet states of CoH<sup>+</sup>.<sup>b</sup>

State of CoH <sup>+</sup>	Ionization	IP(eV)		$\Delta R_e(a_0)^c$	$\Delta\omega_e(\text{cm}^{-1})^d$
		Basis A	Basis B		
$X^4\Phi$	$6\sigma \rightarrow \infty$	7.21	7.23	-0.01	100
$1^4\Pi$	$6\sigma \rightarrow \infty$	7.45	7.53	0.04	15
$1^4\Delta$	$3\Pi \rightarrow \infty$	7.75	7.87	0.15	-105
$2^4\Pi^e$	$1\delta \rightarrow \infty$	9.10	9.16	0.01	5
$2^4\Phi$	$7\sigma \rightarrow \infty$ vertical <sup>f</sup>	9.98			
	$7\sigma \rightarrow \infty$ adiabatic	9.39		1.36	-1180

<sup>a</sup>  $R_e(X^3\Phi) = 2.91 a_0$ ;  $\omega_e(X^3\Phi) = 1925 \text{ cm}^{-1}$  (Refs. 18 and 21).

<sup>b</sup> For ionic states calculated at  $R = 3.0 a_0$  (basis A) and  $R = 2.9 a_0$  (basis B).

<sup>c</sup>  $\Delta R_e = R_e(\text{CoH}^+) - R_e(\text{CoH}, X^3\Phi)$ .

<sup>d</sup>  $\Delta\omega_e = \omega_e(\text{CoH}^+) - \omega_e(\text{CoH}, X^3\Phi)$ .

<sup>e</sup> Left minimum.

<sup>f</sup> This transition is expected to break up the Co-H bond (see the text).

The  $1\delta$  ionization relative to  $1\delta^3 3\pi^3 6\sigma^2 7\sigma^2(X^3\Phi)$  generates the configuration  $B1$  of CoH<sup>+</sup>. According to Table V and Sec. V A, this configuration predominates in  $2^4\Pi$  but also contributes to  $1^4\Pi$ . Accordingly,  $1\delta$  ionization should lead to a prominent line around 9.16 eV (or  $\sim 9.50$  eV corrected) due to  $2^4\Pi$  and a satellite peak ( $1^4\Pi$ ) placed about 1.60 eV below it.

On the other hand, ejection of an electron from the bonding  $7\sigma$  MO leads, as expected, to fragmentation of CoH<sup>+</sup>. In fact, vertical ionization from  $7\sigma^2$  generates  $2^4\Phi(1\delta^3 3\pi^3 6\sigma^2 7\sigma)$ , a state lying (at  $R = 2.90 a_0$ ) about 2.80 eV above  $X^4\Phi$ , or equivalently, being about 0.20 eV less stable than its dissociation limit (channel II). Due to the strong nonadiabatic interaction between  $X^4\Phi$  and  $2^4\Phi$  near  $4.5 a_0$  (Fig. 1 and Sec. V A),  $7\sigma$  ionization may generate the dissociation products Co<sup>+</sup> ( $^5F, d^8$ ) and Co<sup>+</sup> ( $^5F, d^7s$ ) (Table II).

Besides the quartet states discussed above, photoionization from  $X^3\Phi(\text{CoH})$  should be a powerful technique to create selected doublet states of CoH<sup>+</sup>. For instance, the states  $1^2\Phi$ ,  $1^2\Pi$ , and  $2^2\Pi$  all have a significant contribution from the configuration  $A1$ , so that  $6\sigma$  ionization generates (in addition to a low energy PES into  $X^4\Phi$  and  $1^4\Pi$ ) a second region lying 1.40 to 2.00 eV above the quartets due to the aforementioned doublet states.

Similarly,  $3\pi$  ionization leads to the relatively high-lying  $2^2\Delta(C1)$  state, less stable than  $1^4\Delta(C1)$  by about 2.50 eV (Table V). In close analogy with the  $X^3\Phi \rightarrow 1^4\Delta$  ionization band, a short vibrational progression is expected for the transition  $X^3\Phi \rightarrow 2^2\Delta$  due to the similarity between the spectroscopic parameters of both upper ionic states (Table VI).

At this point it is worth recalling that low-lying Rydberg states of neutral species resemble particular ionic states in structure and relative stabilities. For instance, such a behavior has been found to work quite well for the MeH hydrides ScH, TiH, and VH.<sup>5,17</sup> Earlier MRD-CI computations pointed out the similarity between molecular (MeH) and atomic (Me) term values. Certainly, one can estimate the excitation energies of MeH (Rydberg) states by sub-

tracting atomic term values from the respective IPs assigned to ionic states having the same electronic structure as the core of the Rydberg states under consideration.

In the present case a  $5s$  term value of  $2.4 \pm 0.10$  eV has been reported for the  $^4F, ^6F(d^7 4s 5s)$  states of the Co atom.<sup>16</sup> Therefore, based on a recommended IP of 7.50 to 7.60 eV for the transition  $X^3\Phi(\text{CoH}) \rightarrow X^4\Phi(\text{CoH}^+)$ , the Rydberg states  $^{3,5}\Phi(1\delta^3 3\pi^3 6\sigma 7\sigma^2 5s)$  of CoH should lie slightly above 5.0 eV. Along the same line of reasoning, the excitation  $3\pi \rightarrow 5s$  relative to  $X^3\Phi$  should generate the states  $^{3,5}\Delta(1\delta^3 3\pi^2 6\sigma^2 7\sigma^2 5s)$ , a multiplet predicted to lie  $\sim 0.60$  eV above the  $^{3,5}\Phi$  Rydberg states from above. No Rydberg states of CoH have been observed experimentally.<sup>18</sup>

## X. SUMMARY AND CONCLUSIONS

The potential curves, spectroscopic parameters, electronic structure and dissociation energies of several doublet and quartet states of CoH<sup>+</sup>, as well as the ionization potentials of CoH, have been investigated with highly correlated MRD-CI wave functions. The most relevant features are summarized below.

The four low-lying states of CoH<sup>+</sup>, placed in the region from 0 to 0.60 eV, appear in the ordering  $X^4\Phi < 1^4\Sigma^- < 1^4\Pi < 1^4\Delta$ , in agreement with recent predictions from Schilling *et al.*<sup>17</sup> Though these states correlate with the first dissociation channel Co<sup>+</sup> ( $d^8, ^3F$ ) + H( $s, ^2S$ ), they have an equilibrium structure  $d^7 7\sigma^2$  closely related to that of the second and third atomic limits  $^5F$  and  $^3F$  of Co<sup>+</sup> ( $d^7s$ ) + H [both channels with a  $^4F(d^7)$  coupling]. The switching between the molecular configurations  $d^8 7\sigma$  (channel I) and  $d^7 7\sigma^2$  (channels II and III), taking place in the region from 4.0 to 4.5  $a_0$ , particularly affects the behavior of all second quartet  $\Phi$ ,  $\Sigma^-$ ,  $\Pi$ , and  $\Delta$  states. The  $X^4\Phi$ ,  $1^4\Sigma^-$ ,  $1^4\Pi$ , and  $1^4\Delta$  potential curves are little affected because such interactions occur at approximately 1.5 eV above their minima and, as shown in Figs. 1 and 3, the aforementioned potential curves show a regular behavior in the whole range of geometries considered.

At short  $R$ , the states  $2^4\Sigma^-$  and  $2^4\Pi$  (with excitation

energies between 1.6 and 1.9 eV) also arise from  $d^7 7\sigma^2$  configurations, in this case related to a  $^4P(d^7)$  coupling. Since the minima of these  $d^7$  states lie slightly below the first  $d^8$  dissociation limit, their potential curves are strongly perturbed along the dissociation path (Figs. 1 and 3). The  $2^4\Pi$  state shows a potential barrier near  $3.7 a_0$  due to mixing between the bonding and antibonding configurations  $d^7[{}^4P]7\sigma^2$  and  $d^8[{}^3F]7\sigma$ , or equivalently, due to an avoided crossing between 2 and 3  $^4\Pi$  in that region. Besides, close to  $4.5 a_0$  the  $2^4\Pi$  potential curve has a second, shallow minimum caused by mixing between  $d^8[{}^3F]7\sigma$  and  $d^7[{}^4F]7\sigma^2$  (or equivalently, as a result of an avoided crossing in that region between the antibonding  $2^4\Pi$  and the bonding  $1^4\Pi$  states).

One  $2^4\Sigma^-$  state shows similar interactions as the ones pointed out above for  $2^4\Pi$ , yet they are not strong enough to cause the existence of a second minimum in the  $2^4\Sigma^-$  potential curve.

At short distances, the  $2^4\Phi$  and  $2^4\Delta$  potential curves are strongly repulsive, a feature in line with the antibonding character of their leading  $d^8 7\sigma$  configurations. However, mixing between  $d^8 7\sigma$  ( $2^4\Phi$ ,  $2^4\Delta$ ) and  $d^7 7\sigma^2$  ( $X^4\Phi$ ,  $1^4\Delta$ ) gradually increases with nuclear separation, finally leading to a shallow minimum for both states near  $4.0 a_0$  (Figs. 1 and 3). At large  $R$ ,  $2^4\Phi$  and  $2^4\Delta$  are  $d^7$ -like states, as expected by the structure of their dissociation limit  $\text{Co}^+(d^7 s, {}^5F) + \text{H}$ .

Several doublet states are found to be bound. The lowest  $1^2\Delta$  state, arising from the configuration  $1\delta^3 3\pi^4 6\sigma^2$ , is the only bound state of  $d^8$  character with a  $3d\sigma(6\sigma)$ -type of CoH bonding. All other bound states (doublets or quartets) show mainly  $4s(7\sigma)$  type of bonding, as reflected by  $R_e$  values ranging from 2.91 to  $3.05 a_0$ , compared with  $R_e(1^2\Delta) = 2.73 a_0$ .

Since atomic  $\text{Co}^+(d^7 s)$  states with an internal  $^2X(d^7)$  coupling lie about 2.0 eV higher than those with a  $^4X(d^7)$  coupling, the corresponding doublet states  $d^7 7\sigma^2$  of  $\text{CoH}^+$  are also located at higher energies (above 1.60 eV). The potential curves of all doublet states investigated (except  $1^2\Delta$ ) are expected to have significant potential barriers beyond  $R = 5.0 a_0$ , especially for the third channel states  $2^2\Pi$  and  $2^2\Delta$  (Fig. 5).

The ground state dissociation energy  $D_0$  is computed to be 2.06 eV, comparing well with earlier experimental and theoretical data, all close to 2.0 eV.

The photoelectron spectrum of  $\text{CoH}(X^3\Phi, 1\delta^3 3\pi^3 6\sigma^2 7\sigma^2)$  is expected to be instrumental for the spectroscopic characterization of selected low-lying states of  $\text{CoH}^+$ . In a similar manner, an excited  $^5\Phi$  state of neutral CoH was detected recently via the photodetachment spectrum of  $\text{CoH}^-(X^4\Phi)$ .<sup>21</sup>

The PES should contain bands extending from approximately 7.50 to 8.20 eV due to ionization from  $6\sigma$  ( $X^4\Phi$ ,  $1^4\Pi$ ) and  $3\pi$  ( $1^4\Delta$ ). Ejection of an electron from  $1\delta$  of  $X^3\Phi$  (CoH) is predicted to occur near 9.50 eV ( $2^4\Pi$ ), with the possible existence of a satellite peak close to 8.0 eV due to  $1^4\Pi$ . Photons with an energy of about 10.3 eV should

lead to dissociation of  $\text{CoH}^+$  into  $\text{Co}^+ + \text{H}$  since they can eject an electron of the bonding  $7\sigma$  MO.

Combining the present theoretical IPs with the experimental term values of the Rydberg states of Co, we are able to predict that the Rydberg states  $6\sigma \rightarrow 7s$  ( $^3,^5\Phi$ ) and  $3\pi \rightarrow 5s$  ( $^3,^5\Delta$ ) of CoH, for example, lie at about 5.15 and 5.65 eV, respectively.

## ACKNOWLEDGMENTS

Calculations were carried out at the Computing Centre of the University of New Brunswick. This support, as well as support by NSERC (Canada), is gratefully acknowledged.

- <sup>1</sup> See, for example (a) G. D. Byrd, R. C. Burnier, and B. S. Freiser, *J. Am. Chem. Soc.* **104**, 3565 (1982); (b) R. Houriet, L. F. Halle, and J. L. Beauchamp, *Organometallics* **2**, 1818 (1983); (c) S. J. Babinec and J. Allison, *J. Am. Chem. Soc.* **106**, 7718 (1984); (d) N. Aristov and P. B. Armentrout, *ibid.* **108**, 1806 (1986), and references therein.
- <sup>2</sup> (a) M. A. Tolbert and J. L. Beauchamp, *J. Am. Chem. Soc.* **106**, 8117 (1984); (b) N. Aristov and P. B. Armentrout, *ibid.* **106**, 4065 (1985); (c) P. B. Armentrout, L. F. Halle, and J. L. Beauchamp, *ibid.* **103**, 6501 (1981); (d) L. F. Halle, F. S. Klein, and J. L. Beauchamp, *ibid.* **106**, 2543 (1984).
- <sup>3</sup> T. J. Carlin, L. Sallans, C. J. Cassady, D. B. Jacobson, and B. S. Freise, *J. Am. Chem. Soc.* **105**, 6320 (1983).
- <sup>4</sup> J. L. Elkind and P. B. Armentrout, *J. Phys. Chem.* **90**, 6576 (1986).
- <sup>5</sup> (a) J. Anglada, P. J. Bruna, S. D. Peyerimhoff and R. J. Buenker, *J. Molec. Struct. Theochem.* **93**, 299 (1983); (b) **107**, 163 (1984); (c) P. J. Bruna and J. Anglada, in *Quantum Chemistry: The Challenge of Transition Metals and Coordination Chemistry*, edited by A. Veillard (Reidel, Dordrecht, 1986) p. 67; (d) J. Anglada, P. J. Bruna, and S. D. Peyerimhoff (to be submitted); (e) J. Anglada, Ph.D. thesis, Barcelona, Spain, 1985.
- <sup>6</sup> (a) A. E. Alvarado-Swaisgood and J. F. Harrison, *J. Phys. Chem.* **92**, 2757 (1988); (b) A. E. Alvarado-Swaisgood, J. Allison, and J. F. Harrison, *J. Phys. Chem.* **89**, 2517 (1985).
- <sup>7</sup> (a) J. B. Schilling, W. A. Goddard III, and J. L. Beauchamp, *J. Am. Chem. Soc.* **108**, 582 (1986); (b) *J. Phys. Chem.* **91**, 5616 (1987).
- <sup>8</sup> L. G. M. Pettersson, C. W. Bauschlicher, S. R. Langhoff, and H. Partridge, *J. Chem. Phys.* **87**, 481 (1987); D. P. Chong, S. R. Langhoff, C. W. Bauschlicher, S. Walch, and H. Partridge, *ibid.* **85**, 2850 (1986).
- <sup>9</sup> A. W. J. H. Wachters, *J. Chem. Phys.* **52**, 1033 (1970).
- <sup>10</sup> A. K. Rappé, T. A. Smedley, and W. A. Goddard III, *J. Phys. Chem.* **85**, 2607 (1981).
- <sup>11</sup> S. Huzinaga, *J. Chem. Phys.* **42**, 1293 (1965).
- <sup>12</sup> R. J. Buenker and S. D. Peyerimhoff, *Theor. Chim. Acta* **35**, 33 (1974).
- <sup>13</sup> R. J. Buenker and S. D. Peyerimhoff, *New Horizons of Quantum Chemistry*, edited by P. O. Löwdin and B. Pullman (Reidel, Dordrecht 1983), p. 183.
- <sup>14</sup> P. J. Bruna, S. D. Peyerimhoff, and R. J. Buenker, *Chem. Phys. Lett.* **72**, 278 (1980).
- <sup>15</sup> (a) R. J. Buenker, S. D. Peyerimhoff, and P. J. Bruna, *Computational Organic Chemistry*, edited by I. G. Csizmadia and R. Daudel (Reidel, Dordrecht 1981), p. 55; (b) P. J. Bruna and S. D. Peyerimhoff, *Adv. Chem. Phys.* **67**, 1 (1987).
- <sup>16</sup> C. E. Moore, *Atomic Energy Levels*, Natl. Bur. Stand. (US) (1949).
- <sup>17</sup> J. Anglada, P. J. Bruna, and S. D. Peyerimhoff, *Mol. Phys.* **66**, 541 (1989).
- <sup>18</sup> K. P. Huber and G. Herzberg, *Molecular Spectra and Molecular Structure*, Vol. 4, Constants of Diatomic Molecules (Van Nostrand, Princeton, 1979).
- <sup>19</sup> A. Effio, D. Griller, K. U. Ingold, A. L. J. Beckwith, and A. K. Serelis, *J. Am. Chem. Soc.* **102**, 1736 (1980).
- <sup>20</sup> P. B. Armentrout and J. L. Beauchamp, *J. Am. Chem. Soc.* **103**, 784 (1981).
- <sup>21</sup> A. E. Stevens, C. S. Feigerle, and W. C. Lineberger, *J. Chem. Phys.* **87**, 1549 (1987).